Frictional heat from faulting of the 1999 Chi-Chi, Taiwan earthquake

H. Tanaka,[1] W. M. Chen,[2] C. Y. Wang,[2] K. F. Ma,[2] N. Urata,[1] J. Mori,[3] and M. Ando[4]

Received 23 April 2006; revised 17 July 2006; accepted 31 July 2006; published 30 August 2006.

[1] The frictional heat generated during an earthquake is thought to be a major portion of the total energy release. However, there have been no direct measurements of the heat generated by a large earthquake. We present an estimate of the frictional heat produced by the 1999 Chi-Chi, Taiwan earthquake (Mw 7.6), from temperature anomaly that is measured in a borehole penetrating a large slip region (~10 m) of the fault. A local increase in the temperature profile across the fault is interpreted to be the residual heat generated during the earthquake. Analyses of this temperature anomaly lead to a low estimate of the dynamic shear stress, 0.5 to 0.9 MPa, and the heat produced in the large slip region of the fault, 0.68 to 1.32 $\times$ 10^{17} J. The total frictional energy is estimated as 2.4 to 6.1 $\times$ 10^{17} J, indicating that seismic efficiency is 1 to 3%.
Citation: Tanaka, H., W. M. Chen, C. Y. Wang, K. F. Ma, N. Urata, J. Mori, and M. Ando (2006), Frictional heat from faulting of the 1999 Chi-Chi, Taiwan earthquake, *Geophys. Res. Lett.*, *33*, L16316, doi:10.1029/2006GL026673.

1. Introduction

[2] Past studies of heat flow measurements close to the San Andreas fault provided some information about the frictional heat production of faulting, and led to an ongoing debate about the amount of frictional heat generated by earthquakes and the absolute level of stress that drives the faulting process [*Brune et al.*, 1969; *Lachenbruch and Sass*, 1980; *Scholz*, 2002]. Observations from the recent Chi-Chi, Taiwan, earthquake, which was notable for its large surface and near-surface fault displacements (Figure 1) that were observed along the Chelungpu fault [*Ma et al.*, 1999], present the opportunity to directly measure the heat produced during a single earthquake. This is the best recorded large earthquake, with data from a dense regional array of strong-motion instruments [*Lee et al.*, 2001], so the details of the slip distribution and rupture are well known from numerous studies.

2. Outline of the Drill Core and the Temperature Profile

[3] A borehole was drilled into the northern portion of the fault in the year 2000 (Figure 1) in order to sample the slip zones that had large slip (~10 m) during the earthquake. The fault surface near the drilling site dips about 30°E with a slip vector of 66° [*Ma et al.*, 2001] during the 1999 Chi-Chi, Taiwan, earthquake. The borehole was drilled at an angle of about 50° to the west and penetrated the fault at a drilling depth (depth measured along the inclined drill hole) of around 300 m in January, 2001 [*Tanaka et al.*, 2002].

[4] Fluid loss or gain was not observed during penetration of the fault zone. Distributed fracture zone ranges from 285 to 330 m depth, which contains nine slip zones (Figure 2a). The host rock of the fracture zone is composed of moderately consolidated, siltstone, silty sandstone and alteration of these two, which belongs to Kueichulin Formation (upper Miocene to Pliocene) [*Huang et al.*, 2002]. The silty sandstone is well sorted and mostly composed of quartz, feldspar, muscovite and calcite associated with minor amounts of opaque minerals. The siltstone shows similar mineral composition but contains more phyllosilicates. Slip zones are basically composed of fault gouge and fault breccia [*Tanaka et al.*, 2002; *Heermance et al.*, 2003] (Figure 2b). The fault gouge shows brighter gray in color than host rocks. The boundary between fault gouge and host rock is gradual (arrows in Figure 3a), associated with thin transition zone (<2 mm) from host rock to fault gouge. Mineral grains are more disaggregated with proximity to the slip zone (Figure 3a). Grains in fault gouge are extremely fine to be cryptocrystalline materials (<2 μm) [*Wilson et al.*, 2005], and the maximum size is about 25 μm (Figure 3b). Strong preferred alignments of phyllosilicate minerals are evident within fault gouge layer (Figure 3b). However, microscopic textures indicative of frictional melting, such as spherulitic or dendritic crystal morphology, microlites or grassy matrix [*Magloughlin*, 1992], are hardly observed in the slip zones.

[5] Based on the neutron geophysical logs, *Tanaka et al.* [2002] reported that neutron porosity abruptly increase in the drilling interval between 285 m to 330 m. The interval exactly corresponds to the fracture zone (Figure 2a). Lithology around the interval is rather simple, which is composed of silty sandstone and mudstone. Thus, the change in porosity cannot be explained by difference of the lithology. Furthermore, fracture zones in other intervals did show similar values of porosity with surrounding host rocks, implying these fracture zones were already compacted and/or healed. Thus, the fault zone between 285 to 330 m would be the newest, being fractured during coseismic slip by Chi-chi earthquake.

[6] A temperature profile for the borehole was measured in cased-hole with 20 cm/sec. logging velocity by a thermal logging tool three weeks after completion of drilling, which corresponded to 15 month following the earthquake. Other measurements including pumping or fluid injection were not performed before temperature logging. Unfortunately,

[1]Department of Earth and Planetary Sciences, University of Tokyo, Tokyo, Japan.
[2]Geophysical Research Institute, National Central University, Chung-Li, Taiwan.
[3]Disaster Prevention Research Institute, Kyoto University, Kyoto, Japan.
[4]Research Center for Seismology and Volcanology, Nagoya University, Nagoya, Japan.

0094-8276/06/2006GL026673$05.00

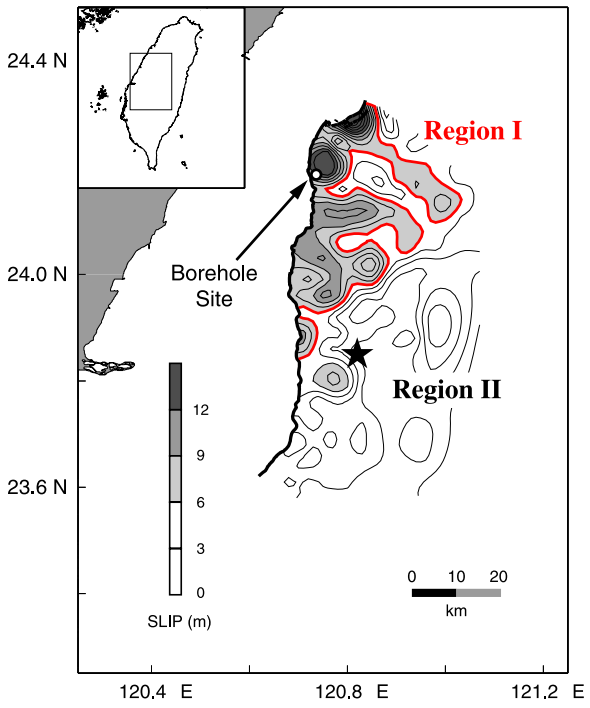

Figure 1. Location of borehole drilled into the Chelungpu fault. Contours show the slip during the 1999 Chi-Chi earthquake from the model *Ji et al.* [2003]. The slip in the region of the borehole was about 9 meters. Large slip portion of the fault at north is denoted as I, and the other region is denoted as II. Star represents the earthquake epicenter. The trace of the faults is shown by the heavy line.

the hole collapsed during open-hole logging, which was conducted right after cased-hole logging. Thus, the hole is no longer accessible. The temperature data for depths of 200 to 400 m are shown in Figure 4. Observed low background geothermal gradient about 5 to 6°C/km compared to those measured at similar depth range in the deeper borehole one year after drilling in 2005 (11°C/km), would be due to incomplete recovery of temperature that lowered by circulation of fluid during drilling.

[7] In Figure 4, a slight rise with double peaks in temperature of about 0.1°C is observed where the temperature profile crosses the fracture zone. The shallower and deeper peaks within positive temperature anomaly exactly correspond to the slip zones A and B. There are two ways of explaining for this observation. One is that the temperature increase is the residual heat from the frictional heating during the earthquake. Another potential source of the local temperature increase in the fracture zone may be thermal disturbance due to outflow of fluids from the slip zones. However, recent results of permeability measurements across the Nojima fault zone indicate that the slip zone is less permeable (around 10^{-19} m^2) than the fracture zone surrounding the slip zone (around 10^{-16} m^2) [*Lockner et al.*, 2000]. Similar results have been reported from many exhumed fault zones containing fault gouge [e.g., *Evans et al.*, 1997; *Tsutsumi et al.*, 2004; *Uehara and Shimamoto*, 2004]. If this is also the case for the Chelungpu fault zone, thermal peaks would be associated with fracture zones. However, the thermal peaks A and B existing right on the thin slip zones suggest that the thermal anomaly would not be generated by fluid flow but by frictional heating.

[8] Due to insufficient recovery of geothermal gradient (6°C/km) compared to those measured one year after drilling of deeper borehole (11°C/km) the detected thermal anomaly may be smaller than intrinsic value. Thus the temperature anomaly in Figure 4 is a minimum value. We estimate the maximum positive thermal anomaly would be about twice (0.2°C) the measured value based on condition of recovery of geothermal gradient.

3. Estimation of Temperature Rise and Frictional Coefficient

[9] For a first order estimate of the heat generated by the earthquake, we assume that the frictional heat generated along slip zones at the time of the earthquake caused observed temperature anomaly and any subsequent heat transfer is due entirely to conduction. We use the solution of one-dimensional conduction in an infinite medium to model the temperature anomaly. The temperature as a function of time (t) and distance (x) from a thin layer is well known [*Officer*, 1974].

$$T(x,t) = \frac{S}{2\sqrt{\pi\alpha t}} e^{-x^2/4\alpha t}, \tag{1}$$

where α is the thermal diffusivity and the strength of the heat source S is,

$$S = \frac{\tau \cdot D}{c \cdot \rho}, \tag{2}$$

where D is the displacement of the fault, c is the specific heat, ρ is the density, and τ is the shear stress. The heat sources were assumed to be the two slip zones A and B observed in the drill cores (Figure 2).

[10] To evaluate equations (1) and (2), we set the time t to be 4.36×10^7 seconds (15 months). The thermal transport properties of fracture zone materials are directly measured using HOT DISK system [*Gustavsson*, 1991; *Gustavsson et al.*, 1995] from a drill core penetrating the Chelungpu fault zone at 1100 m depth in 2004. Due to the narrow thickness of the slip zones, thermal diffusivity data of the surrounding fracture zone were considered: the average value with standard error is $1.47 \pm 0.043 \times 10^{-6}$ m^2/s from 57 data points measured from the depths surrounding the slip zone. The values of specific heat and density were measured from slip zone materials: the average values with standard errors for c and ρ are: c = 326 ± 42.5 J/kgK, and ρ = 2245 ± 58.1 kg/m^3 from the six data from slip zones. We confirmed that the errors did not vary the results significantly. Thus, for simplicity, the approximate values, α; 1.5×10^{-6} m^2/s, c; 300 J/kgK, and ρ; 2200 kg/m^3 were considered for the calculation.

[11] Shear stress and displacements are the parameters to be estimated. We assume that the values of shear stress for the two slip zones are similar, and that the total displacements for the two slip zones are at most 10 m based on the slip inversion [*Ji et al.*, 2003]. A two-dimensional grid search gives the best-fit curves with values τ_A = 0.47 MPa when D_A = 4 m for peak A and τ_B = 0.48 MPa when D_B =

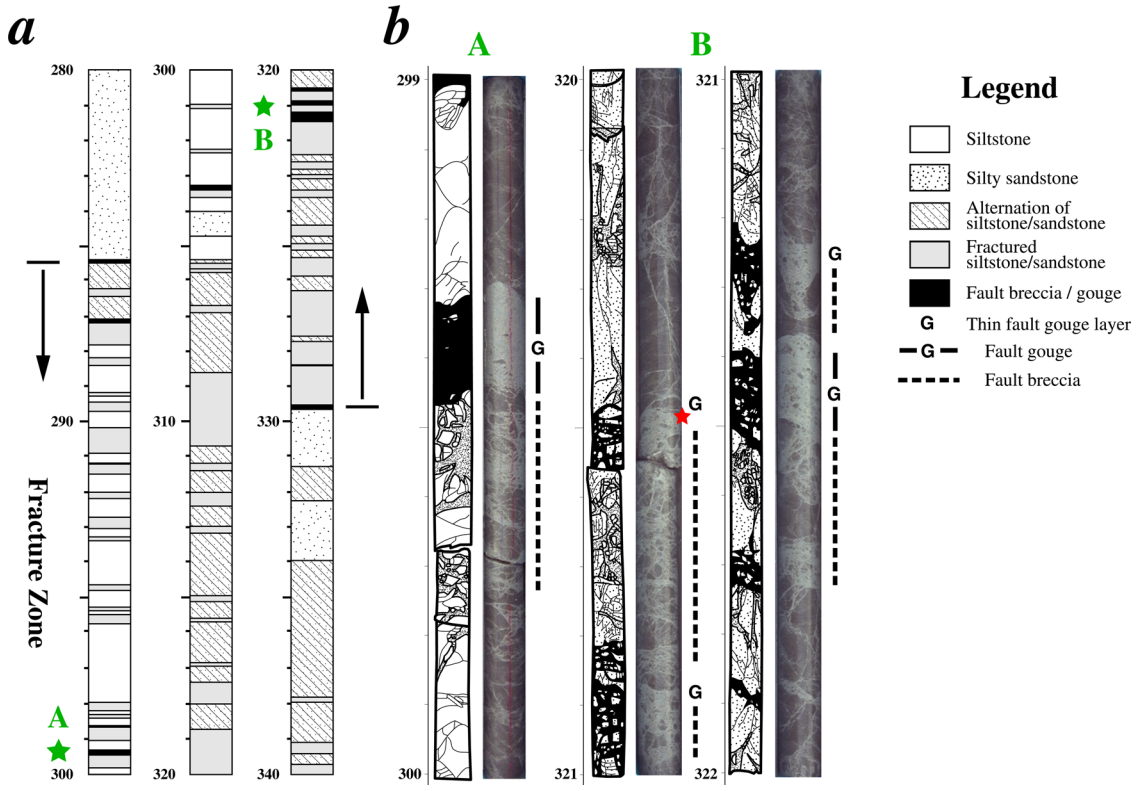

Figure 2. (a) Geological columnar section of drilled core across the fault zone. Slip zones A and B correspond to the two thermal peaks within positive temperature anomaly shown in Figure 4. (b) Occurrence of drill core around slip zone A and B. Slip zones are composed of relatively thin fault gouge and fault breccia. The fault gouge sample is obtained from 325 m depth, which is shown by red star. Microscopic occurrence of the fault gouge is shown in Figure 3.

5 m for peak B. The strengths of the heat sources (S) are 2.1 for peak A and 2.5 for peak B. Even though we assume very narrow slip zone, for example, 1 cm in thickness [*Sibson*, 2003], the temperature rises in slip zones are estimated to be 210°C (A) and 250°C (B), which are insufficiently high to melt silicate materials at shallow crustal conditions. The insufficient temperature rise would explain the fact that few microscopic textures of melting in the gouge layer.

[12] Figure 5 shows the result of calculated temperatures using the value of shear stress, along with the observed data with the linear depth gradient removed. The shear stress doubled (about 0.95 MPa for both slip zones) if the maximum estimate of thermal anomaly is considered. A single peak approximation is also examined. In this case, heat source is located at the center of thermal anomaly (314 m depth), the best-fit curve is obtained with values τ = 0.83 MPa and $\alpha = 3.4 \times 10^{-6}$ m^2/s with 8 m slip. The value of α independently defines the width of diffusion of temperature. Thus, the result is unrealistic because the value of thermal diffusivity is more than double the measured values of fracture zone materials. The results support the interpretation that the thermal anomaly resulted from frictional heating is due to two thin slip zones rather than a single thermal source located within the fracture zone.

[13] Assuming that the normal stress on the fault, σ_n, is equal to the lithostatic stress, σ_l, and that the shear stress on the fault is linearly related to σ_n,

$$\tau = \mu(\sigma_n - \sigma_p), \tag{3}$$

where σ_p is the pore pressure, which is assumed to be the hydrostatic pressure. The coefficient of friction μ is estimated to be 0.13 for slip zone A and 0.12 for slip zone B (Figure 5). Again, the values of μ are doubled if the maximum estimate of thermal anomaly is taken. For reverse fault regimes, the horizontal compressive stress is reported to be 2 to 4 times the vertical stress [*Sibson*, 1974; *Brace and Kohlstedt*, 1980; *Ikeda et al.*, 2001]. For this range of values, the level of friction needed to produce the thermal anomaly is quite low, with μ estimated to be 0.04 to 0.06 using a fault dip of 30°. The extremely low friction behavior might be explained by some current models of dynamic faulting, such as thermal pressurization [*Wibberley and Shimamoto*, 2005], fault lubrication [*Brodsky and Kanamori*, 2001], along with a low value of specific heat of slip zone materials. No apparent microscopic evidence of melting suggests the dynamic weakening mechanisms for this observed large slip and slip velocity of the earthquake rupture.

4. Estimation of Frictional Energy and Energy Budget

[14] As discussed below, based on the slip distribution and analyses of the frequency content of the recorded strong-motion records, the shallow part of the northern portion appears to have ruptured in a different manner from the other portions of the fault during the earthquake [*Ma et al.*, 2003; *Ji et al.*, 2003; *Wu et al.*, 2001]. The large

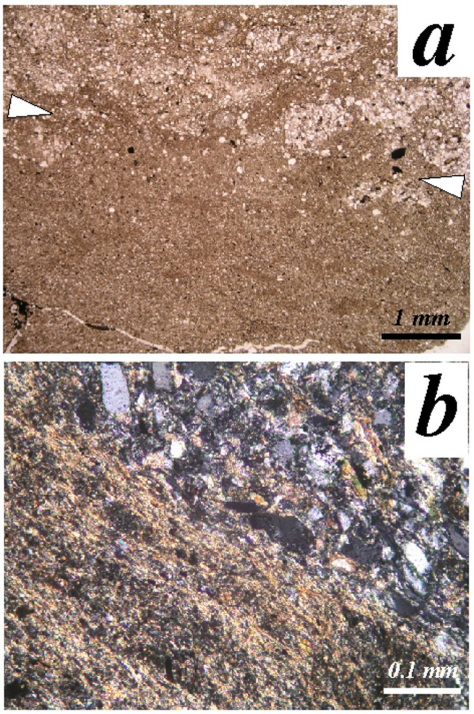

Figure 3. Microscopic occurrence of the fault gouge sampled from the slip layer at 325 m depth. (a) Occurrence of the boundary between host rock and fault gouge under plane polarized light. The boundary is gradual with thin transition zone (2 mm) between the fault gouge and host rock. (b) Magnified view of the fault gouge under crossed polarized light. Phyllosilicate minerals show strong preferred alignments. Fragments in the fault gouge are extremely fine. However, evidence of frictional melting is hardly observed in the fault gouge.

displacements and velocities of the fault in the north (Region I in Figure 1) imply a large fast slip with low levels of friction that produced relatively less high frequency radiation. In contrast, the other portion (Region II in Figure 1) had smaller displacements and may have ruptured with higher frictional values, producing the high acceleration ground motions. Recent high-velocity shear experiments indicate that dynamic friction lowers to around 0.2 for granular quartz-gouge as slip velocity approaches 0.1 m/s [*Toro et al.*, 2004]. Considering that the average slip velocity for region I is approximately 1 m/s and that for region II is 0.5 m/s [*Ji et al.*, 2003], we estimate the total frictional energy for the earthquake. The values of $\mu = 0.12$ and 0.24 (minimum and maximum estimates) ($\sigma_n = \sigma_l$; case 1) and $\mu = 0.05$ and 0.1 ($\sigma_n > \sigma_l$; case 2) are applied to large slip region I and $\mu = 0.2$ (for both cases) for the region II along the ruptured Chelungpu fault. Then, using these values to calculate the shear stress, we estimate the frictional heat, Q_f, for the entire fault using,

$$Q_f = \sum_i \tau_i u_i a_i, \tag{4}$$

where the summation i is over each sub-fault as parameterized in the slip distribution models, τ_i is given by equation (2), and u_i and a_i are the sub-fault slip and area, respectively. We used a slip distribution for the earthquake determined from inversion of local strong-motion data [*Ji et al.*, 2003; *Wu et al.*, 2001]. This calculation results in values for the frictional energy of 6.80×10^{16} J and 1.34×10^{17} (min. and max.) for region I, and 1.62×10^{17} J (case 1) or 4.66×10^{17} J (case 2) for region II.

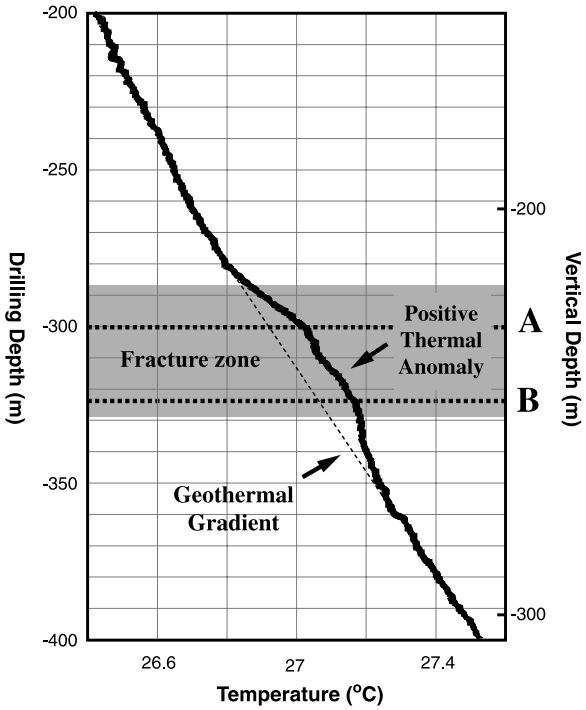

Figure 4. Temperature recorded as function of depth in the borehole. Shaded area shows the fracture zone. A and B in shaded area correspond to the slip zones A and B in Figure 2.

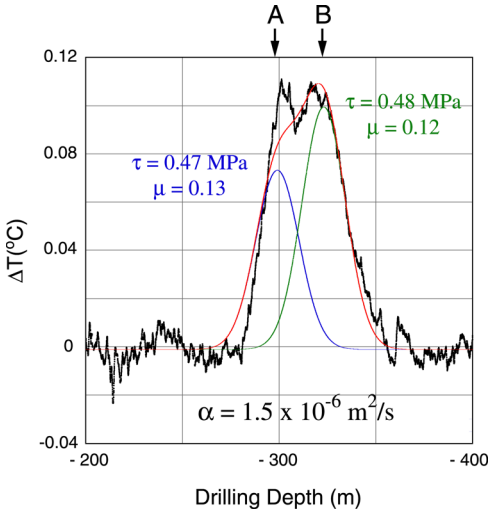

Figure 5. Observed temperature data (heavy dark line) and an example from grid search results for slip zones A (green line) with $D = 4$ m and B (blue line) with $D = 5$ m. Red line shows sum of calculated results of A and B.

[15] In addition to the frictional heat, the other two major parts of the energy balance are the radiated energy of the seismic waves and the fracture energy associated with the rupture. The radiated energy of the seismic waves for this earthquake has been estimated from teleseismic data [*Venkataraman and Kanamori*, 2004] giving a value of 0.66×10^{16} J. The fracture energy is related to the rupture speed for an earthquake [*Fossum and Freund*, 1975]. Source modeling of the Chi-Chi earthquake give rupture speeds of about 0.7 times the shear wave velocity, which corresponds to a ratio of the fracture energy to the radiated energy ratio of 0.6. This results in fracture energy of 0.43×10^{16} J. Combining the frictional heat, radiated energy and fracture energy, the total energy for the earthquake is 2.41 to 6.11×10^{17} J. The ratio of the radiated energy to the total energy gives a seismic efficiency of 1.1% to 2.7%. *Kanamori et al.* [1998] inferred that the maximum seismic efficiency was 3.6% for 1994 Bolivian deep-focus earthquake based on examinations of source parameters. It might be worthy to note that our estimate of seismic efficiency is comparable with their result even though the depths of seismic slips between the two earthquakes are largely different.

[16] There are some uncertainties in this analysis. One of the issues is whether the temperature measurements from shallow depths are representative of the seismic faulting. If not, then the coefficient of friction of 0.05 or 0.12 (or 0.1 to 0.24) may not be representative of the large slip portion of the Chelungpu fault in the north. However, currently this is the only value we have available. Deeper penetration into a fault zone immediately after a large earthquake could contribute to further understanding energy budget of earthquakes.

[17] **Acknowledgments.** We sincerely thank Y. B. Tsai of National Central University for supporting the project during these five years. We appreciate thoughtful suggestions from the anonymous reviewer. We thank H. Ito for his kindly advice for geophysical borehole logging. We also thank A. Sakaguchi, K. and K. Ujiie of JAMSTEC, Japan for extensive support of on-site work of the drilling. R. Geller of the University of Tokyo helped revision of the manuscript. Thanks are extended to many students especially for C. H. Chen, C. B. Lu, H. J. Huang, C. W. Chang and W. N. Wu in National Central University that have been involved in the drilling project. The project was funded mainly by Ministry of Education, Culture, Sports, Science and Technology, Japan and National Science Council, Taiwan.

References

Brace, W. F., and D. L. Kohlstedt (1980), Limits on lithsopheric stress imposed by laboratory experiments, *J. Geophys. Res.*, *85*, 6248–6252.

Brodsky, E., and H. Kanamori (2001), Elastohydrodyanamic lubrication of faults, *J. Geophys. Res.*, *106*, 16,357–16,373.

Brune, J. N., T. L. Henyey, and R. F. Roy (1969), Heat flow, stress, and rate of slip along the San Andreas fault, California, *J. Geophys. Res.*, *74*, 3821–3827.

Evans, J. P., C. B. Forster, and J. V. Goddard (1997), Permeability of fault-related rocks, and implications for hydraulic structure of fault zones, *J. Struct. Geol.*, *19*, 1393–1404.

Fossum, A. F., and L. B. Freund (1975), Nonuniformly moving shear crack model of a shallow focus earthquake mechanism, *J. Geophys. Res.*, *80*, 3343–3347.

Gustavsson, M., N. S. Saxena, E. Karawacki, and S. E. Gustavsson (1995), Specific heat measurement in the hot disk thermal constants analyzer, *Therm. Conductivity*, *23*, 56–65.

Gustavsson, S. E. (1991), Transient plane source technique for thermal conductivity and thermal diffusivity measurements of solid materials, *Rev. Sci. Instrum.*, *62*, 797–804.

Heermance, R., Z. K. Shipton, and J. P. Evans (2003), Fault structure control on fault slip and ground motion during the 1999 rupture of the Chelungpu Fault, Taiwan, *Bull. Seismol. Soc. Am.*, *93*, 1034–1050.

Huang, S. T., J. C. Wu, J. H. Hung, and H. Tanaka (2002), Studies of sedimentary facies, stratigraphy, and deformation structures of the Chelungpu fault zone on cores from drilled wells in Fengyuan and Nantou, Central Taiwan, *Terr. Atmos. Oceanic Sci.*, *13*, 253–278.

Ikeda, R., Y. Iio, and K. Omura (2001), In situ stress measurements in NIED boreholes in and around the fault zone near the 1995 Hyogo-ken Nanbu earthquake, Japan, *Island Arc*, *10*, 252–260.

Ji, C., D. V. Helmberger, D. J. Wald, and K. F. Ma (2003), Slip history and dynamic implications of the 1999 Chi-Chi, Taiwan, earthquake, *J. Geophys. Res.*, *108*(B9), 2412, doi:10.1029/2002JB001764.

Kanamori, H., D. L. Anderson, and T. H. Heaton (1998), Frictional melting during the rupture of the 1994 Bolivian Earthquake, *Science*, *279*, 839–841.

Lachenbruch, A. H., and J. H. Sass (1980), Heat flow and energetics of the San Andreas fault zone, *J. Geophys. Res.*, *85*, 6185–6222.

Lee, W. H. K., T. C. Shin, K. W. Kuo, K. C. Chen, and C. F. Wu (2001), CWB free-field strong-motion data from the 21 September Chi-Chi, Taiwan earthquake, *Bull. Seismol. Soc. Am.*, *91*, 1370–1376.

Lockner, D. A., H. Naka, H. Tanaka, H. Ito, and R. Ikeda (2000), Permeability and strength of core samples from the Nojima Fault of the 1995 Kobe Earthquake, in *Proceedings of the International Workshop on the Nojima Fault Core and Borehole Data Analysis*, *U.S. Geol. Surv. Open File Rep. 00-129*, 147–152.

Ma, K. F., C. T. Lee, Y. B. Tsai, T. C. Shin, and J. Mori (1999), The Chi-Chi, Taiwan earthquake: Large surface displacements on an inland thrust fault, *Eos Trans. AGU*, *80*, 605.

Ma, K. F., J. Mori, S. J. Lee, and S. B. Yu (2001), Spatial and temporal distribution of slip for the 1999 Chi-Chi, Taiwan earthquake, *Bull. Seismol. Soc. Am.*, *91*, 1069–1087.

Ma, K., E. E. Brodsky, J. Mori, C. Ji, T. A. Song, and H. Kanamori (2003), Evidence for fault lubrication during the 1999 Chi-Chi, Taiwan, earthquake (Mw7.6), *Geophys. Res. Lett.*, *30*(5), 1244, doi:10.1029/2002GL015380.

Magloughlin, J. F. (1992), Microstructural and chemical changes associated with cataclasis and frictional melting at shallow crustal levels: The cataclasite-pesudotachylyte connection, *Tectonophysics*, *204*, 243–260.

Officer, C. B. (1974), *Introduction to Theoretical Geophysics*, Springer, New York.

Scholz, C. H. (2002), The debate on the strength of crustal fault zones, in *The Mechanics of Earthquakes and Faulting*, pp. 158–167, Cambridge Univ. Press, New York.

Sibson, R. H. (1974), Frictional constraints on thrust, wrench and normal faults, *Nature*, *249*, 542–544.

Sibson, R. H. (2003), Thickness of the seismic slip zone, *Bull. Seismol. Soc. Am.*, *93*, 1169–1178.

Tanaka, H., C. Y. Wang, W. M. Chen, A. Sakaguchi, K. Ujiie, H. Ito, and M. Ando (2002), Initial science report of shallow drilling penetrating into the Chelungpu fault zone, Taiwan, *Terr. Atmos. Oceanic Sci.*, *13*, 227–251.

Toro, G. D., D. L. Goldsby, and T. E. Tullis (2004), Friction falls towards zero in quartz rock as slip velocity approaches seismic rates, *Nature*, *427*, 436–439.

Tsutsumi, A., S. Nishino, K. Mizoguchi, T. Hirose, S. Uehara, K. Sato, W. Tanikawa, and T. Shimamoto (2004), Principal fault zone width and permeability of the active Neodani fault, Nobi fault system, southwest Japan, *Tectonophysics*, *379*, 93–108.

Uehara, S., and T. Shimamoto (2004), Gas permeability evolution of cataclasite and fault gouge in triaxial compression and implications for changes in fault-zone permeability structure through the earthquake cycle, *Tectonophysics*, *378*, 183–195.

Venkataraman, A., and H. Kanamori (2004), Effect of directivity on estimates of radiated seismic energy, *J. Geophys. Res.*, *109*, B04301, doi:10.1029/2003JB002548.

Wibberley, C. A. J., and T. Shimamoto (2005), Earthquake slip weakening and asperities explained by thermal pressurization, *Nature*, *436*, 689–692.

Wilson, B., Z. Reches, and J. Brune (2005), Particle size and energetics of gouge from earthquake rupture zones, *Nature*, *434*, 749–752.

Wu, C., M. Takeo, and S. Ide (2001), Source process of the Chi-Chi Earthquake: A joint inversion of strong motion data and global positioning system data with a multifault model, *Bull. Seismol. Soc. Am.*, *91*, 1128–1143.

M. Ando, Research Center for Seismology and Volcanology, Nagoya University, Nagoya 464-8602, Japan.

W. M. Chen, K. F. Ma, and C. Y. Wang, Geophysical Research Institute, National Central University, Chung-Li 320-54, Taiwan.

J. Mori, Disaster Prevention Research Institute, Kyoto University, Kyoto 611-0011, Japan.

H. Tanaka and N. Urata, Department of Earth and Planetary Sciences, University of Tokyo, Tokyo 113-003, Japan. (tanaka@eps.s.u-tokyo.ac.jp)